Reversal of Stathmin-Mediated Microtubule Destabilization Sensitizes Retinoblastoma Cells to A Low Dose of Antimicrotubule Agents: A Novel Synergistic Therapeutic Intervention

Moutushy Mitra,[1,2] *Mallikarjuna Kandalam,*[1] *Curam S. Sundaram,*[3] *Rama Shenkar Verma,*[4] *Uma K. Maheswari,*[2] *Sethuraman Swaminathan,*[2] *and Subramanian Krishnakumar*[1]

Purpose. To explore the possibility of stathmin as an effective therapeutic target and to evaluate the synergistic combination of stathmin RNAi and the antimicrotubule agents paclitaxel and vincristine to retinoblastoma Y79 cells.

Methods. RNAi-mediated specific inhibition of stathmin expression in Y79 cells was shown by real-time quantitative RT-PCR (RT-Q-PCR), its effect on cell proliferation by MTT assay, cell invasion using matrigel, microtubule polymerization by immunohistochemistry, apoptosis, cell cycle analysis by flow cytometry analysis, and the changes in FOXM1 protein expression were studied by Western blot. The effect of combination treatment of stathmin siRNA and paclitaxel/vincristine was studied by assessing cell viability and apoptosis.

Results. Short interfering RNA–mediated transient stathmin downregulation resulted in a marked inhibition of retinoblastoma cell proliferation and cell invasion in vitro. Stathmin inhibition promoted Y79 cells to G2/M phase, and ultimately there were increased apoptotic events as evidenced by higher caspase-3 activation and cleaved poly-(ADP-ribose) polymerase expression. Cells transfected with stathmin siRNA showed long and bundled microtubule polymers and sensitized the Y79 cells significantly to paclitaxel and vincristine.

Conclusions. Stathmin may be a pivotal determinant for retinoblastoma tumorigenesis and chemosensitivity. Strategies to inhibit stathmin will help to enhance the cytotoxic effect of paclitaxel while reducing toxicity (or side effects) to normal cells caused by high doses. (*Invest Ophthalmol Vis Sci.* 2011; 52:5441–5448) DOI:10.1167/iovs.10-6973

From the [1]Department of Ocular Pathology, Vision Research Foundation, Sankara Nethralaya, Tamil Nadu, India; [3]Proteomics Facility, Center for Cellular and Molecular Biology, Hyderabad, India; [4]Indian Institute of Technology, Madras, India; and [2]Centab, Shanmugha Arts, Science, Technology and Research Academy University, Tanjore, India.

Supported by DBT Grants BT/PR7968/MED/14/1206/2006 and BT/PR7152/MED/14/961/2006.

Submitted for publication November 30, 2010; revised February 5, 2011; accepted March 28, 2011.

Disclosure: **M. Mitra**, None; **M. Kandalam**, None; **C.S. Sundaram**, None; **R.S. Verma**, None; **U.K. Maheswari**, None; **S. Swaminathan**, None; **S. Krishnakumar**, None.

Corresponding author: Subramanian Krishnakumar, Department of Ocular Pathology, Vision Research Foundation, Sankara Nethralaya, No. 18 College Road, Nungambakkam, Chennai 600006, India; drkrishnakumar_2000@yahoo.com.

Taxanes and vinca alkaloids are antimicrotubule drugs that are commonly used chemotherapeutic drugs.[1] Taxanes stabilize microtubules, and vinca alkaloids destabilize microtubules[1,2] Both classes of drugs promote cell death by affecting microtubule dynamics, thereby interfering with the function of the mitotic spindle and inducing apoptosis by promoting mitotic arrest.[3,4] Antimicrotubule drugs are among the most effective drugs in the treatment of breast cancer.[5] Vincristine, a vinca alkaloid, is being routinely given to retinoblastoma patients as a combination therapy with DNA-damaging agents such as carboplatin and etoposide.[6] Recently, Fernando et al[7] has shown that paclitaxel is effective when given as monotherapy to reduce retinal tumor burden. Although taxanes significantly inhibit proliferation and induce apoptosis of retinoblastoma cells, toxic effects related to high doses is observed in xenograft models.[7] Paclitaxel delivered in combination with other therapeutic agents would result in a greater tumor response and would reduce the associated toxicities.[8] One of the important principles of combination chemotherapy is to include combinations of chemotherapeutic drugs with antisense strategies that target specific proteins whose expression is necessary for the malignant phenotype.

Recently, Mallikarjuna et al.[9] reported that stathmin, an 18-kDa phosphoprotein, is highly expressed in primary retinoblastoma tumors. Stathmin, also known as oncoprotein 18, prosolin, p19, 19K, p18, and op18, is a conserved cytosolic protein that plays a critical role in mitosis and possibly other cellular processes.[10,11] Stathmin has been shown to regulate the dynamics of the microtubules that make up the mitotic spindle, a role associated with carcinogenesis that indicates that stathmin is one of the fundamental cancer-associated genes and a potential target for diagnosis and treatment.[12,13] Stathmin overexpression leads to resistance to antimicrotubule agents, including altered drug binding and delayed transit from the G2 to the M phase.[14] Decreased sensitivity of vinca alkaloids and taxol to breast cancer cells caused by the overexpression of the microtubule-associated protein stathmin was reported by Alli et al.[14,15]

The purpose of the present study was to explore the possibility of stathmin as an effective therapeutic target and to evaluate the effect of stathmin inhibition on the chemosensitivity of retinoblastoma cells to paclitaxel and vincristine in vitro.

Methods

Cell Lines, Cell Culture, and Drugs

Y79 cell line was obtained from the Cell Bank, RIKEN BioResource Center (Ibaraki, Japan). Rosewell Park Memorial Institute (RPMI) 1640

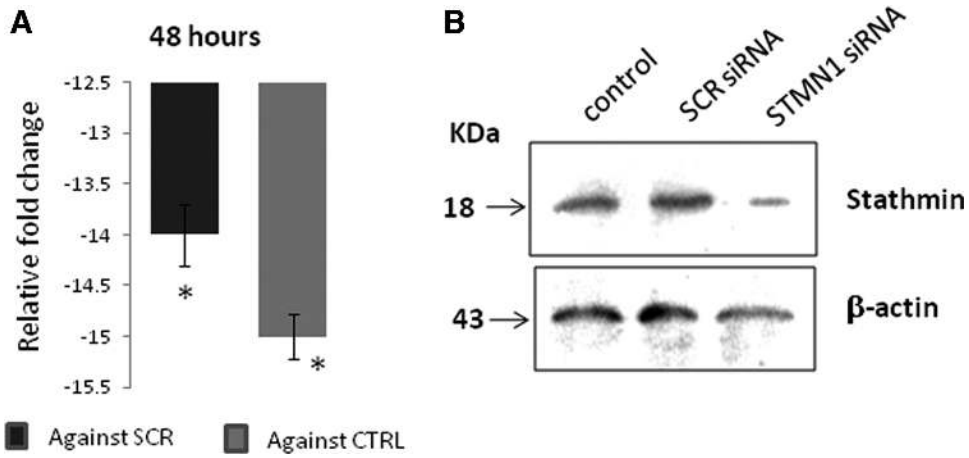

Figure 1. (**A**) Graph shows the downregulation of stathmin mRNA levels in Y79 cells treated with stathmin siRNA for 48 hours against untransfected and scrambled siRNA (*$P < 0.05$). (**B**) Western blotting shows the marked decrease in the band intensity of the Y79 cells treated with stathmin siRNA for 48 hours compared to untransfected and scrambled siRNA treatments.

media and fetal bovine serum (FBS) were purchased from Gibco-BRL (Rockville, MD). Y79 was cultured in RPMI 1640 medium supplemented with 10% heat-inactivated fetal calf serum, 0.1% ciprofloxacin, 2 mM L-glutamine, 1 mM sodium pyruvate, and 4.5% dextrose and grown in suspension at 37°C in a 5% CO_2 humidified incubator. Paclitaxel (T7191) and vincristine (V8879) were purchased from Sigma Aldrich (Saint Louis, MO). This study was conducted at the Medical Research Foundation and Vision Research Foundation, Sankara Nethralaya, India, and was approved by the Vision Research Foundation ethics board.

siRNA and Transfection

The short interfering RNAs (siRNAs) were purchased from Qiagen (Santa Clarita, CA). Gene silencing of stathmin expression was performed essentially as described previously using sequence-specific siRNA and transfection reagents.[16] Briefly, 100,000 cells were plated in each well of 6-well plates and allowed to grow for 24 to 36 hours (until they were 40–60% confluent). siRNA was then transfected into cells at a concentration of 100 nM using lipofectamine reagent according to manufacturer protocol. Human stathmin siRNA (catalog no. SI00301875) and scrambled siRNA (catalog no. 1022563) were used in this study.

Combination Treatment with Stathmin siRNA

Scrambled control or stathmin siRNA was transfected into cells as described above. After 48 hours, cells were treated with vehicle or increasing concentrations of the appropriate drug for 72 hours.

Mitogenic Assay

Cell viability of Y79 cells treated with the appropriate drug or siRNA alone or in combination was determined by a standard (3-(4,5-Dimethylthiazol-2-yl)-2,5-diphenyltetrazolium bromide (MTT)–based colorimetric assay (Invitrogen, Carlsbad, CA). Reagents were mixed and added to each well (10 μL/well), plates were incubated for 3 hours at 37°C in a cell culture incubator, and the color intensity was measured at 490 nm using a microplate reader. The antiproliferative effect of different treatments was calculated as a percentage of cell growth with respect to the respective control.

Assessment of Apoptosis by Flow Cytometry

The induction of apoptosis by paclitaxel and vincristine in combination with stathmin siRNA or in the free form was studied by flow cytometry using annexin FITC apoptosis detection kit (BD Biosciences, San Jose, CA). For apoptosis study, the cells were pelleted and then resuspended in 100 μL of 1× binding buffer (Clontech Laboratories, Inc., Palo Alto, CA). Thereafter, 5 μL Annexin V-FITC (final concentration, 1 μg/mL; BD Biosciences) and 5 μL propidium iodide (10 μg/μL; MP Biomedicals, Inc., Heidelberg, Germany) were added to the cells and incubated at room temperature in the dark for 20 minutes. Before flow cytometric analysis, 400 μL of 1× binding buffer were added to the cells and the extent of apoptosis was determined by analyzing 15,000 ungated cells using a fluorescence-activated cell sorting (FACS) flow cytometer (FACScalibur) and Cell Quest software (both from Becton-Dickinson, San Jose, CA). All experiments were performed in triplicate.

Cell Cycle Analysis

Cell cycle analysis was studied by flow cytometry using BD cycle test plus DNA Reagent kit (BD Biosciences, Heidelberg, Germany) according to the manufacturer's protocol. In brief, after specific incubation period cells were centrifuged for 5 minutes at 300*g* at room temperature and 1 mL buffer solution was added to the supernatant, the cells

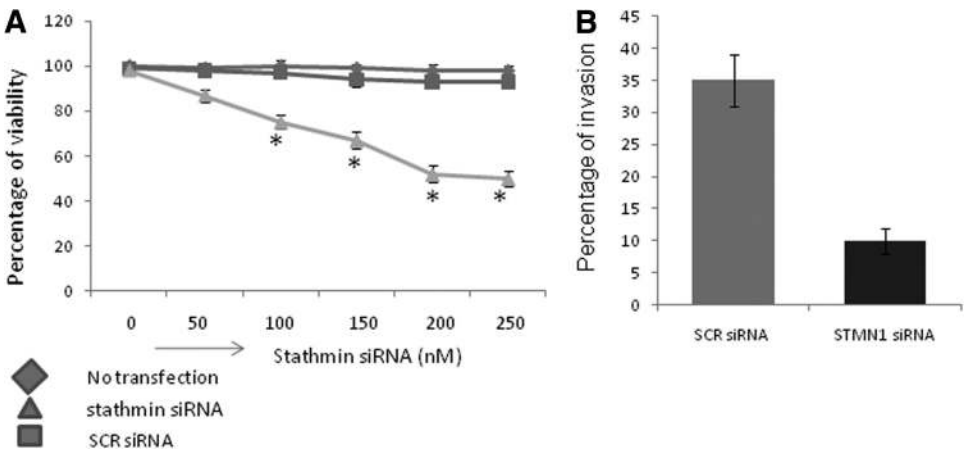

Figure 2. (**A**) Graph showing the effect of stathmin inhibition on cell viability of Y79 cells. There is a dose-dependent decrease in the cell viability in response to increasing concentrations of stathmin siRNA (*$P < 0.05$). (**B**) Bar diagram shows the significant reduction in the percentage of Y79 cell invasion in the matrigel experiments after treatment with stathmin siRNA for 48 hours.

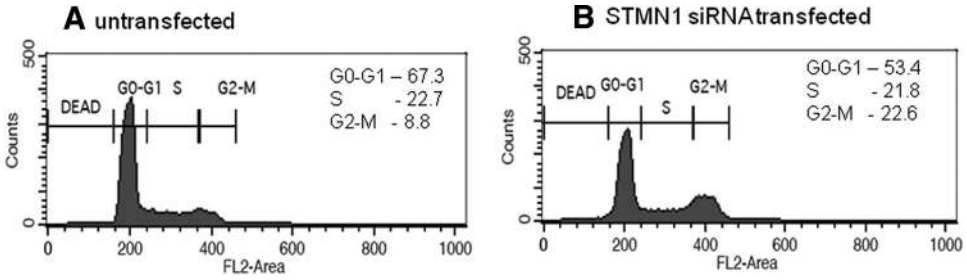

FIGURE 3. Cell cycle analysis shows the significant accumulation of Y79 cells in the G2-M phase after treatment with stathmin siRNA for 48 hours. (**A**) Untransfected control. (**B**) Stathmin siRNA–treated.

were suspended by gentle vortexing at low speed (this procedure was repeated twice). Solution A (250 μL) was added and mixed by tapping and was incubated for 10 minutes. Next, 200 μL of solution B was added and mixed by tapping and was incubated for 10 minutes. Finally, 200 μL cold solution of C (PI) was added to each tube, mixed by tapping, and then incubated for 10 minutes in the dark on ice. The sample was filtered through a 35-μm cell strainer and analyzed with a flow cytometer.

Mitotic Index

Cells were collected and centrifuged onto glass slides and then fixed and stained with 10 g/mL 4,6-diamidino-2-phenylindole (Sigma-Aldrich) in PBS containing 5 μg/mL RNase A (Bangalore Genei, Bangalore, India). For each sample, 200 cells were randomly counted by fluorescence microscopy. Mitotic figures were scored blindly.

Caspase-3 and PARP Activity Assay by Flow Cytometer

For intracellular staining, cells were fixed and permeabilized with 2% paraformaldehyde and 0.05% Tween 20 to allow intracellular labeling with respective cleaved poly(ADP-ribose) polymerase (PARP) antibody (ab32064; Abcam, Cambridge, UK) and cleaved caspase-3 antibody (Cell Signaling Technology, Danvers, MA; 1:200) was added and the cells were incubated for 1 hour. After incubation, the cells were washed twice with ice cold PBS and incubated with secondary FITC anti-rabbit immunoglobulin G (Sigma;1:1000 dilution) for 30 minutes at 40°C. The cells were then washed twice with ice cold PBS was resuspended in FACS buffer and analyzed by FACS.

In Vitro Cell Invasion Analysis

The 24-well plate Transwell system with a polycarbonate filter membrane of 8-mm pore size (Corning; Lowell, MA) was used. The cell suspensions were seeded to the upper compartment of the Transwell chamber at the cell density of 1×10^5 in 100 μL serum free medium. After 24 hours, the medium was removed and the filter membrane was fixed with 4% formalin for 1 hour. The opposite surface of the filter membrane that faced the lower chamber was stained with methylene blue for 3 minutes and the migrated cells were then visualized under an inverted microscope.

Quantitative RT-PCR

Total RNA was extracted with TRIzol reagent (Invitrogen) and purified by RNeasy MinElute Cleanup kit (QIAGEN, Valencia, CA) according to the manufacturers' instructions. Quantitative RT-PCR was carried out using one-step quantitative RT-PCR kit for SYBR green I (Eurogentec, San Diego, CA) with 100 ng of RNA template per reaction. Controls included reactions free of reverse transcriptase and RNA template. Each reaction was carried out in triplicate. The cDNA from the untreated Y79 cells or cells treated with scrambled siRNA was used as control for quantifying the stathmin gene expression in the cells treated with stathmin siRNA. Tubes without template cDNA were included as negative control for quantitative PCR. For stathmin, 40 cycles and an annealing temperature of 58°C was used with 5′-ATGGCTTCTTCTGATATCCAG-3′ and antisense 5′- TTAGTCAGCTTCAGTCTCGTC-3′ set of primers. Commercial software (SDS version 1.3; ABI) was used to calculate $\Delta\Delta$Ct relative expression values for stathmin normalized to the glyceraldehyde 3-phosphate dehydrogenase endogenous control.

Western Blotting

Cells were lysed in 300 μL ice cold lysis buffer (50 mM Tris-HCl, 5 mM EDTA, 150 mM NaCl, 0.1% SDS, 1% Nonidet, 1 mM protease inhibitor cocktail). Whole-cell lysates were resolved by 12% SDS polyacrylamide gel electrophoresis, transferred to nitrocellulose membrane, blocked, and probed with the appropriate antibody. Protein was detected by horseradish peroxidase-conjugated secondary antibody and enhanced chemiluminescence kit (Amersham, Pittsburgh, PA). Antibodies included antistathmin (dilution, 1:500; Santa Cruz Biotechnology), anti-actin (Sigma-Aldrich), anti-α-tubulin (dilution, 1:500; Santa Cruz Biotechnology) and anti-FOXM1 (dilution, 1:400; Santa Cruz Biotech-

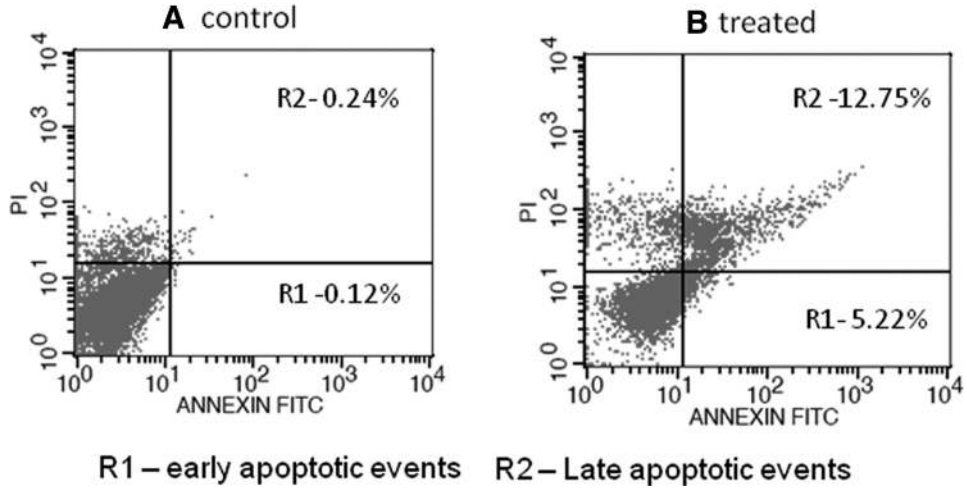

FIGURE 4. Flow cytometry dot plot shows the increase in early and late apoptotic events in response to stathmin inhibition. (**A**) Untransfected. (**B**) stathmin siRNA treated.

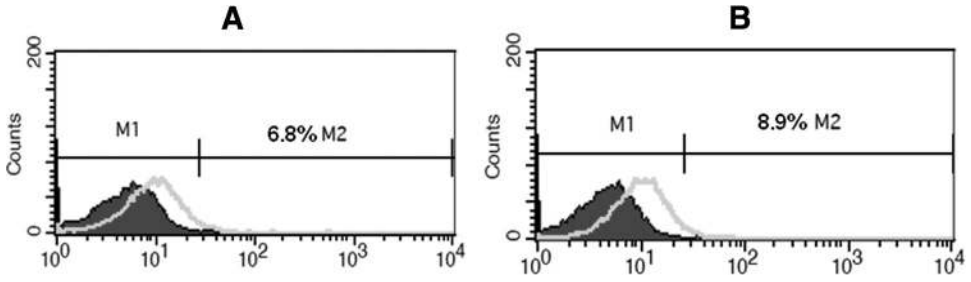

FIGURE 5. Flow cytometry density plot shows the increase in caspase-3 activity and cleaved PARP activity in the cells treated with stathmin siRNA. (**A**) Caspase-3 positivity. (**B**) PARP positivity.

nology) Densitometry was carried out using Image J software (developed by Wayne Rasband, National Institutes of Health, Bethesda, MD; available at http://rsb.info.nih.gov/ij/index.html). Each experiment was performed in triplicate.

Immunohistochemistry Staining of Microtubules

Cells grown in tissue culture chamber slides were transfected with 100 nM siRNA, fixed with methanol, blocked with 3% bovine serum albumin, and stained with α-tubulin polyclonal antibody (Santa Cruz Biotechnology) as the primary antibody at a dilution of 1:100 and incubated for 12 hours at 4°C. After primary antibody incubation, the reaction was developed using Novolink polymer kit and hematoxylin was used for counter staining. Isotypic antibodies were used for negative control staining. The fixed Y79 cell block stained for α-tubulin on the slides were interpreted using light microscopy (Nikon, Melville, NY).

Statistical Analysis

All experiments were repeated at least three times. Independent *t*-test analysis was used for statistical analysis. The differences were considered significant for P values of < 0.05.

RESULTS

Downregulation of Stathmin by siRNA in Y79 Cells

We transiently transfected Y79 cell line with siRNA targeting stathmin. Real-time RT-PCR (Fig. 1A) and Western blot analyses (Fig. 1B) were used to determine the effect of treatment with siRNA on stathmin expression at the mRNA and protein levels in Y79 cell line. As shown in Figure 1A, treatment of Y79 cells with 200 nM stathmin siRNA for 48 hours reduced stathmin mRNA levels by 14-fold and 15-fold against scrambled siRNA ($P < 0.05$) and controls ($P < 0.05$), respectively. As shown in Figure 1B, stathmin protein levels were reduced by twofold after 48 hours of siRNA treatment.

Effects of RNA Interference Targeting Stathmin on Cell Proliferation and Cell Invasion

To analyze phenotypic changes, we first investigated the effects of transient stathmin siRNA on cellular proliferation of retinoblastoma cells. Cell proliferation was evaluated by MTT assay daily for various concentrations of stathmin siRNA.

As shown in Figure 2A, treatment of Y79 cells with stathmin siRNA resulted in a reduced cell proliferation by 50% at 250 nM, These results showed that siRNA-mediated transient stathmin downregulation resulted in marked inhibition of retinoblastoma cell proliferation in vitro.

The in vitro matrigel Transwell invasion assay revealed that the invasion potential of stathmin expressing Y79 cells markedly decreased after 48 hours of siRNA-mediated stathmin inhibition ($P < 0.05$; Fig. 2B).

Effect of RNA Interference Targeting Stathmin on Cell Cycle, Apoptosis and Mitotic Parameters

The proliferation inhibition of Y79 cells by knockdown of stathmin expression was caused by disrupting the cell cycle and affecting microtubule assembly shown in other types of mammalian cells.[17,18] To reveal the mechanisms underlying RNAi-mediated proliferation inhibition, we used flow cytometric analysis to detect changes in the cell cycle and quantify apoptotic rates in Y79 cells. We first analyzed the DNA contents of cell populations after transient transfection of stathmin siRNA at the concentration of 200 nM into Y79 cells. After 72 hours of siRNA treatment, the population of G2/M phase was significantly increased and the population of G1/G0 phase was obviously decreased ($P = 0.005$) compared to untransfected cells (Fig. 3).

Next, an annexin V-fluorescein isothiocyanate apoptosis detection kit (BD Biosciences) was used to detect cell apoptosis of stathmin siRNA transfected Y79 cells. Cell apoptosis analysis by flow cytometry showed that compared with untransfected Y79 cells, the apoptosis rate of stathmin siRNA

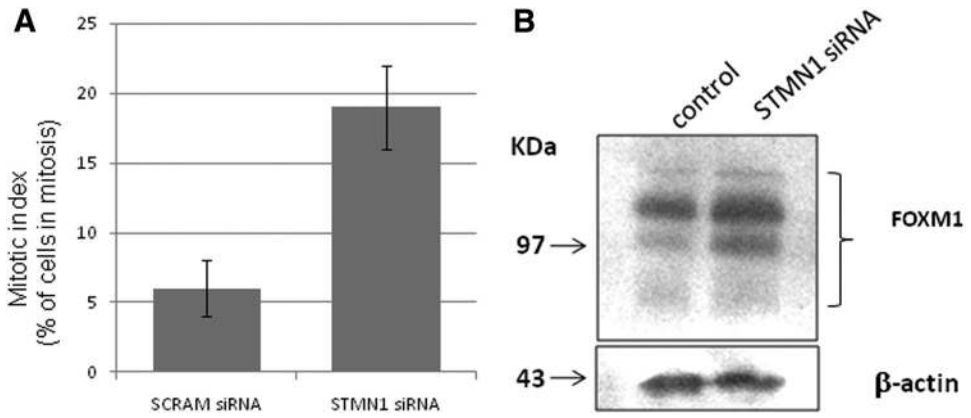

FIGURE 6. (**A**) Bar diagram shows the increase in the mitotic figures of the Y79 cells treated with stathmin siRNA. (**B**) Western blot shows the increase in the intensity of FOXM1 expression in the cells treated with stathmin siRNA compared to untransfected cells.

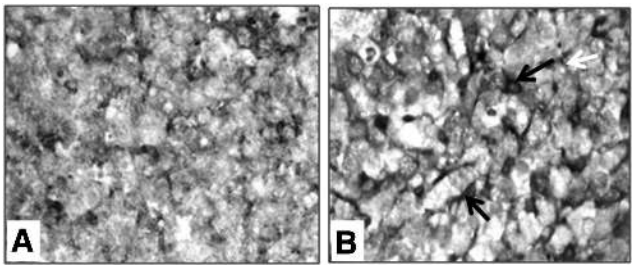

FIGURE 7. Immunohistochemistry showing the microtubule polymerization patterns in the Y79 cells (fixed after siRNA treatment) treated with stathmin siRNA. (**A**) Y79 cells without transfection. (**B**) Y79 cells transfected with stathmin siRNA.

treated cells significantly increased by 17.9% ± 2.3 ($P < 0.05$; Fig. 4). Flow cytometry analysis showed 6.8% of caspase-3 (Fig. 5A) and 8.9% PARP positivity (Fig. 5B) in the Y79 cells treated with stathmin siRNA.

To analyze the distribution of cells in mitosis, we determined the mitotic index in stathmin siRNA transfectants compared with that of scrambled siRNA transfected controls. Figure 6A shows that stathmin siRNA transfectants had higher cells entering mitosis than the control cell lines. In addition, we show that the Y79 cells treated with stathmin siRNA had a 1.7-fold higher FOXM 1 expression compared to the cells without siRNA transfectants (Fig. 6B).

All above results suggested that RNAi-mediated transient or stable downregulation of stathmin expression in Y79 cells could induce cell accumulation in the G2/M phase and final apoptosis.

Effect of Silencing Stathmin on Microtubule Polymerization

Stathmin inhibition affects the distribution of cells throughout the cell cycle through microtubule polymerization. Stathmin destabilizes microtubules and promotes depolymerization. Therefore, to reverse the destabilizing effect of stathmin on microtubules, we tested the ability of RNA interference to knock down stathmin expression and induce microtubule polymerization. Y79 cells were transfected with stathmin siRNA (nontoxic concentration), scrambled control siRNA, and/or transfection reagent alone, and assayed for α tubulin staining patterns by immunohistochemistry. To analyze the microtubule network, transfected cells were fixed and permeabilized to allow free tubulin to diffuse from the cell, and stained with antitubulin and FITC-conjugated secondary antibody to visualize tubulin polymer. Cells transfected with stathmin siRNA had long and bundled microtubule polymers (Fig. 7A), whereas cells transfected with scrambled-control siRNA showed short and diffuse microtubule polymers (Fig. 7B).

Dose-Dependent Decrease in Cell Proliferation of Y79 Cells Treated with Paclitaxel and Vincristine

We observed a dose-dependent decrease of Y79 cell viability by MTT assay on treatment with paclitaxel and vincristine with an IC50 of 3.5 nM and 1 nM, respectively (Figs. 8A and B). Flow cytometry analysis showed 12% of caspase-3 with 18% PARP activation and 13.2% of caspase-3 with 16.2% of PARP activation in the Y79 cells treated with 0.5 nM of paclitaxel and vincristine. respectively (Fig. 9A–D).

Effects of RNA Interference Targeting Stathmin on Drug Sensitivity

Because of the effects of silencing stathmin on microtubule polymerization described above, we sought to determine whether or not silencing stathmin could increase sensitivity to antimicrotubule agents. Y79 cells were transfected with 200 nM stathmin siRNA or scrambled control siRNA, and analyzed for sensitivity to paclitaxel and vincristine by MTT assay. Y79 cells transfected with stathmin siRNA were 10-fold more sensitive to paclitaxel (Fig. 10A) and twofold more sensitive to vincristine (Fig. 10B) than cells transfected with scrambled control siRNA. Cell apoptosis analysis by flow cytometry showed that Y79 cells transfected with stathmin siRNA showed 50.16% of apoptosis (29.42% of early apoptosis, 20.74% of late apoptosis) with paclitaxel (Fig. 11A) and of 49.89% apoptosis (26.46% of early apoptosis, 23.43% of late apoptosis) with vincristine (Fig. 11B). Without treatment with stathmin siRNA, Y79 cells showed 29.96% of apoptosis (12.99% of early apoptosis, 16.97% of late apoptosis) with paclitaxel (Fig. 11C) and 14.53% of apoptosis (5.97% early apoptosis and 8.56% late apoptosis) with vincristine (Fig. 11D).

Increased Caspase-3 Activation and PARP Cleavage in Y79 Cells After Combination Treatment with Stathmin siRNA and Paclitaxel/Vincristine

Stathmin siRNA transfectants showed significantly higher cells positive for active caspase-3 and cleaved PARP (26.2% and 24.8%) in the Y79 cells treated with paclitaxel (Figs. 12A–B). Stathmin siRNA transfectants showed significantly higher cells positive for active caspase-3 and cleaved PARP (30.8% and 38.2%) in the Y79 cells treated with vincristine than untransfectants (Figs. 12C–D).

DISCUSSION

In the present study to explore the possibility of stathmin as an effective therapeutic target, we used an RNA interference tech-

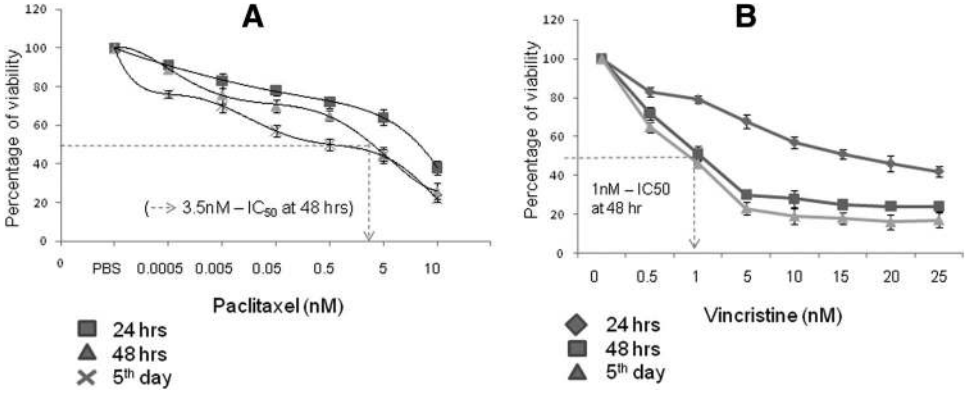

FIGURE 8. Graph shows the cell viability of Y79 cells treated with various increasing concentrations of paclitaxel and vincristine for 24 hours, 48 hours, and 5 days. (**A**) Paclitaxel. (**B**) Vincristine.

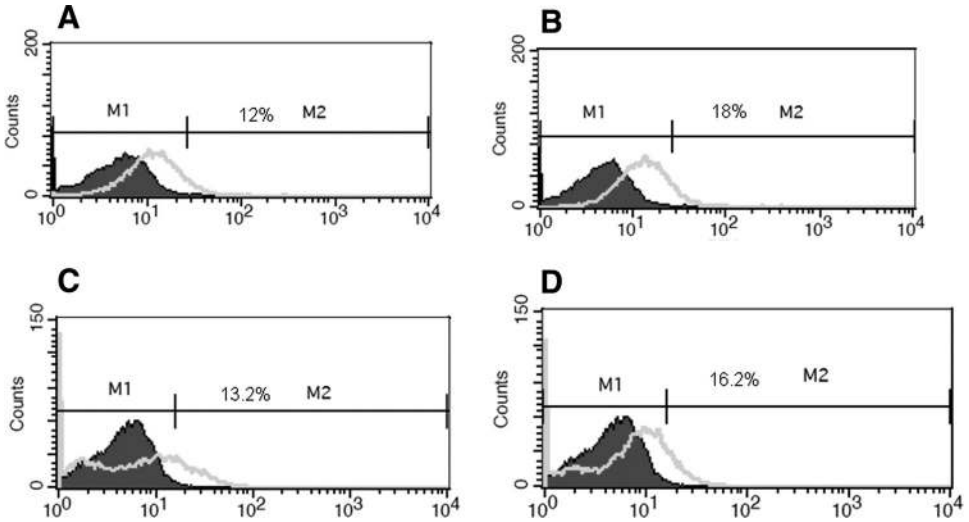

FIGURE 9. Cell cycle analysis showing the caspase-3 and PARP positivity in the Y79 cells treated with paclitaxel and vincristine. (**A**) Caspase-3 in paclitaxel-treated cells. (**B**) PARP in paclitaxel-treated cells. (**C**) PARP in vincristine-treated cells. (**D**) PARP in vincristine-treated cells.

nique to silence endogenous stathmin expression in retinoblastoma cell lines. We observed that transient stathmin downregulation in retinoblastoma cells reduce proliferation potential and invasion potential in vitro. We also detected increased apoptosis rates of stathmin siRNA transfectants compared to control cells. All these results suggest that stathmin may be an important molecule involved in the proliferation and invasion of retinoblastoma tumor cells and a potential target for suppressing proliferation and triggering apoptosis, which can be explained by its key roles in mitosis. We have reasons to believe that stathmin may provide an excellent molecular target for retinoblastoma therapy.

We evaluated the effect of stathmin expression on the sensitivity of retinoblastoma cell lines to antimicrotubule drugs and found that targeting stathmin expression can induce microtubule polymerization or G2-M progression, respectively, and sensitize stathmin-overexpressing retinoblastoma cells to paclitaxel and vincristine. Because stathmin participates in the control of microtubule polymerization,[8] we determined its effect in retinoblastoma cells by comparing the content of polymerized microtubules as a function of stathmin expression. We showed that stathmin expression correlates inversely with microtubule polymerization. Similar results were obtained by Wang et al.,[8] who found that overexpression of stathmin in breast cancer cells decreased staining of the microtubule network. The precise mechanism by which stathmin decreases microtubule polymer mass is complex. Data to support a role of stathmin in promoting microtubule "catastrophe" as well as in sequestering tubulin dimers exist.[16,19–21] The polymerization state of microtubules can affect the binding and increased chemosensitivity of antimicrotubule drugs, which is evidenced by increased expression of active caspase-3 and cleaved PARP in the present study. We found that increased polymerization caused by stathmin inhibition increases the sensitivity of retinoblastoma cells to low dose of paclitaxel (Fig. 10A).

To understand the mechanism by which stathmin inhibition leads retinoblastoma cells more sensitive to vincristine, we focused on the effects of stathmin expression on the distribution of cells throughout the cell cycle. We found that stathmin inhibition increases the number of cells in G2-M as measured by flow cytometry (Fig. 3B) and obviously increases the number of cells in mitosis as measured by counting mitotic figures (Fig. 6A). When Y79 cells were treated with stathmin siRNA, there was a significant increase in FOXM1 expression when we stained with an antibody that recognizes several proteins that are phosphorylated at the onset of mitosis[22,23] (Fig. 6B).

Therefore, overexpression of stathmin appears to reduce the cytotoxic effects of vincristine by impeding progression of cells from G2 into mitosis. In support of this interpretation, Alli et al.[15] found that G2-M checkpoint control increased the sensitivity to both vinca alkaloids and taxanes. We agree with the hypothesis put forth by Alli et al.[15] that "the mechanism of stathmin-induced resistance to paclitaxel can be explained by both decreased drug binding to a diminished microtubule polymer mass and decreased entry into mitosis. The effects of stathmin on vinblastine resistance occur despite increased drug binding and are attributable to decreased entry of treated cells into mitosis."

Our findings suggest that stathmin may be an important target protein involved in retinoblastoma tumorigenesis and

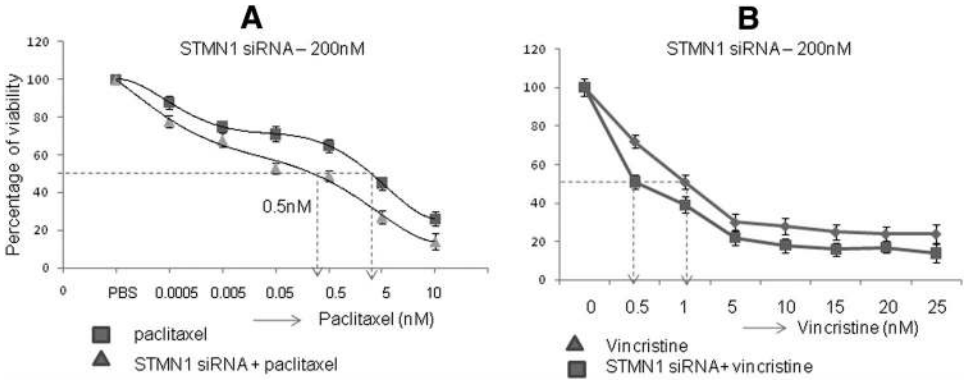

FIGURE 10. Graph shows the cell viability of Y79 cells treated with combination of stathmin siRNA and paclitaxel/vincristine. (**A**) Stathmin siRNA plus paclitaxel. (**B**) Stathmin siRNA plus vincristine.

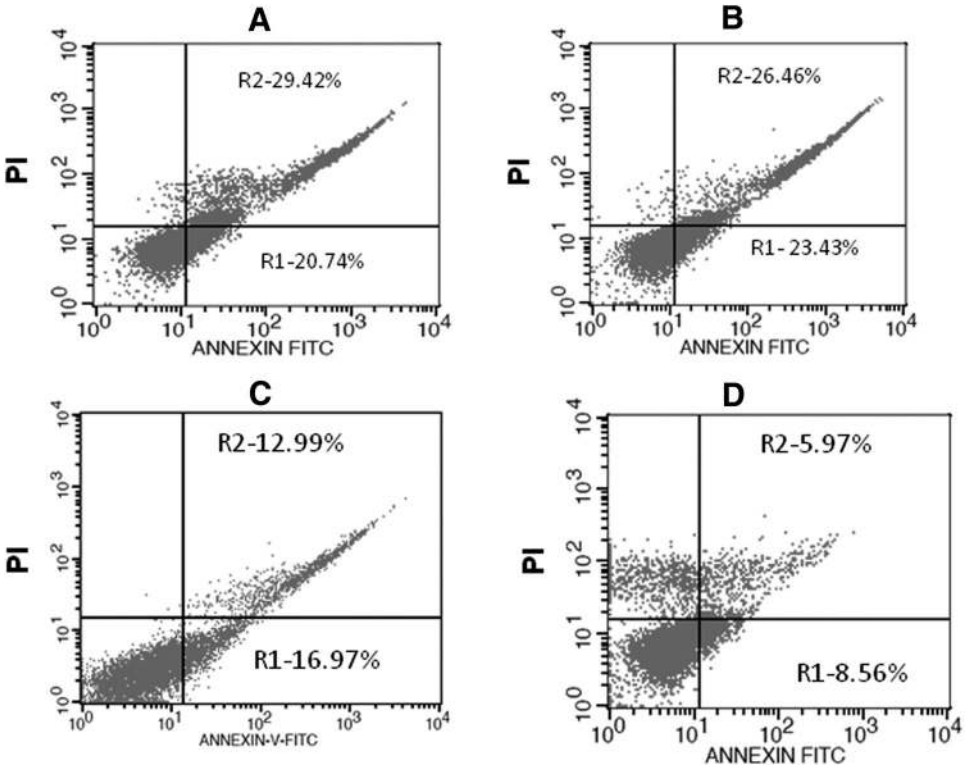

FIGURE 11. Flow cytometry graph showing the increased early and late apototic events in the cells treated with paclitaxel or vincristine in individual or in combination of stathmin siRNA and paclitaxel/vincristine. (**A**) Stathmin siRNA plus paclitaxel. (**B**) Stathmin siRNA plus vincristine. (**C**) Paclitaxcel. (**D**) Vincristine.

chemosensitivity, so it is expected to be a potential therapeutic target for the treatment of retinoblastoma. An approach to inhibit stathmin may help to augment the cytotoxic effect of paclitaxel while reducing toxicity to normal tissues caused by high doses. Vincristine in combination with other drugs is a standard treatment for retinoblastoma. Understanding the effects of stathmin in the clinical setting may have important implications for the outcome of therapy. We conclude that RNAi-mediated stathmin silencing synergizes with paclitaxel and vincristine exposure to make use of more potent antiproliferative and antitumor effects.

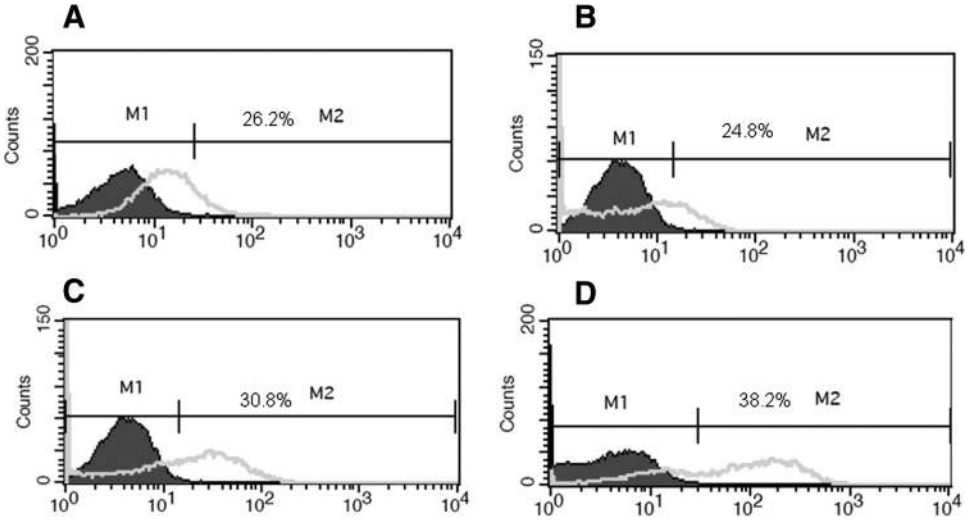

FIGURE 12. Flow cytometry plot showing the increased caspase-3 and PARP positivity in the Y79 cells treated with combination of stathmin siRNA and paclitaxel/vincristine. (**A**) Caspase-3 in paclitaxel plus stathmin siRNA–treated cells. (**B**) PARP in paclitaxel plus stathmin siRNA–treated cells. (**C**) Caspase-3 in vincristine plus stathmin siRNA–treated cells. (**D**) PARP in vincristine plus stathmin siRNA–treated cells.

Acknowledgments

The authors thank the Core Lab Faculty Staff (Central Instrumentation Facility, Vision Research Foundation, Chennai, India) for handling the flow cytometry experiments.

References

1. Dumontet C, Sikic BI. Mechanisms of action of and resistance to antitubulin agents: microtubule dynamics, drug transport, and cell death. *J Clin Oncol.* 1999;17:1061–1070.
2. Giannakakou P, Sackett D, Fojo T. Tubulin/microtubules: still a promising target for new chemotherapeutic agents. *J Natl Cancer Inst.* 2000;92:182–183.
3. Malawista SE, Sato H, Bensch KG. Vinblastine and griseofulvin reversibly disrupt the living mitotic spindle. *Science.* 1968;160:770–772.
4. Beck WT, Cass CE, Houghton PJ. Microtubule-targeting anticancer drugs derived from plants and microbes: vinca alkaloids, taxanes, and epothilones. In: Bast RC, Kufe DW, Pollack RE et al, eds. *Cancer Medicine.* 5th ed. London: B.C. Decker, Inc.; 2000:680–697.
5. DeVita V. Principles of cancer management: chemotherapy. In: DeVita VT, Hellman S, Rosenberg SA, eds. *Cancer Principles and Practice of Oncology.* 5th ed. Philadelphia: Lippincott-Raven; 1997:333–347.
6. Rodriguez-Galindo C, Chantada GL, Haik BG, Wilson MW. Treatment of retinoblastoma: current status and future perspectives. *Curr Treat Options Neurol.* 2007;9:294–307.
7. Suárez F, Jockovich ME, Hernandez E, Feuer W, Parel JM, Murray TG. Paclitaxel in the treatment of retinal tumors of LH beta-Tag murine transgenic model of retinoblastoma. *Invest Ophthalmol Vis Sci.* 2007;48:3437–3440.
8. Wang R, Dong K, Lin F, et al. Inhibiting proliferation and enhancing chemosensitivity to taxanes in osteosarcoma cells by RNA interference-mediated downregulation of stathmin expression. *Mol Med.* 2007;13:567–575.
9. Mallikarjuna K, Sundaram CS, Sharma Y, et al. Comparative proteomics analysis of differentially expressed proteins in primary retinoblastoma tumors. *Proteomics Clin Appl.* 2010;4:449–463.
10. Belmont LD, Mitchison TJ. Identification of a protein that interacts with tubulin dimmers and increases the catastrophe rate of microtubules. *Cell.* 1996;84:623–631.
11. Laird AD, Shalloway D. Oncoprotein signaling and mitosis. *Cell Signal.* 1997;9:249–255.
12. Murphy ME, Cassimeris L. A novel cancer therapy approach targeting microtubule function. *Cancer Biol Ther.* 2006;5:1721–1723.
13. Mistry SJ, Atweh GF. Role of stathmin in the regulation of the mitotic spindle: potential applications in cancer therapy. *Mt Sinai J Med.* 2002;69:299–304.
14. Alli E, Yang JM, Ford JM, Hait WN. Reversal of stathmin-mediated resistance to paclitaxel and vinblastine in human breast carcinoma cells. *Mol Pharmacol.* 2007;71:1233–1240.
15. Alli E, Bash-Babula J, Yang JM, Hait WN. Effect of stathmin on the sensitivity to antimicrotubule drugs in human breast cancer. *Cancer Res.* 2002;62:6864–6869.
16. Belmont LD, Mitchison TJ. Identification of a protein that interacts with tubulin dimers and increases the catastrophe rate of microtubules. *Cell.* 1996;84:623–631.
17. Gao P, Lin F. Inhibitory effects of stathmin gene SiRNA on cultured HeLa cell lines. *J Modern Oncol.* 2006;2:210–212.
18. Zhang HZ, Wang Y, Gao P, et al. Silencing stathmin gene expression by survivin promoter-driven siRNA vector to reverse malignant phenotype of tumor cells. *Cancer Biol Ther.* 2006;5:1457–1461.
19. Andersen SS. Spindle assembly and the art of regulating microtubule dynamics by MAPs and stathmin/Op18. *Trends Cell Biol.* 2000;10:261–267.
20. Holmfeldt P, Larsson N, Segerman B, et al. The catastrophe-promoting activity of ectopic op18/stathmin is required for disruption of mitotic spindles but not interphase microtubules. *Mol Biol Cell.* 2001;12:73–83.
21. Howell B, Deacon H, Cassimeris L. Decreasing oncoprotein 18/stathmin levels reduces microtubule catastrophes and increases microtubule polymer in vivo. *J Cell Sci.* 1999;112:3713-3722.
22. Westendorf JM, Rao PN, Gerace L. Cloning of cDNAs for M-phase phosphoproteins recognized by the MPM2 monoclonal antibody and determination of the phosphorylated epitope. *Proc Natl Acad Sci U S A.* 1994;91:714–718.
23. Davis FM, Tsao TY, Fowler SK, Rao PN. Monoclonal antibodies to mitotic cells. *Proc Natl Acad Sci U S A.* 1983;80:2926-2930.